

Backbone Curvature in Polythiophenes

Ralph Rieger, Dirk Beckmann, Alexey Mavrinskiy, Marcel Kastler, and Klaus Müllen*

Max Planck Institute for Polymer Research, Ackermannweg 10, 55128 Mainz, Germany

Received June 5, 2010. Revised Manuscript Received July 20, 2010

A series of five polymers containing different benzodithiophene isomers copolymerized with alkylated dithiophene have been synthesized and characterized in terms of their semiconducting properties. Because of the different bonding geometry of the benzodithiophene monomers, a varying degree of curvature is introduced into the polymer backbone chain. The influence of this curvature on the solubility, the electronic levels, the morphology in a film, and the charge carrier mobility in organic field-effect transistors has been investigated. It turns out that an increased degree of curvature improves the solubility, but decreases the order in the film. As a result, the polymer with an intermediate degree of curvature yields the highest charge-carrier mobilities. These findings shall serve as guideline for the rational design of other semiconducting polymers.

Introduction

The prospect for lightweight, cost-effective, and large-scale production of electronic devices has stimulated an enormous interest in organic semiconductors.^{1,2} The materials available at the moment document the promise of this endeavor, but organic semiconductors do not yet satisfy all requirements for device production.^{3,4,5} From a practical point of view, it has turned out that conjugated polymers are most promising for large-scale production.⁶ They readily form homogeneous films from solution, enabling printing techniques such as inkjet or gravure printing.^{7,8} In comparison to small molecules such as pentacene or rubrene, however, polymers do not yet show comparably high mobilities in field-effect transistors. To increase the mobility but still retain the advantage of easy solution processing, we synthesized polymers with new monomer building blocks and tested them in transistors.⁹

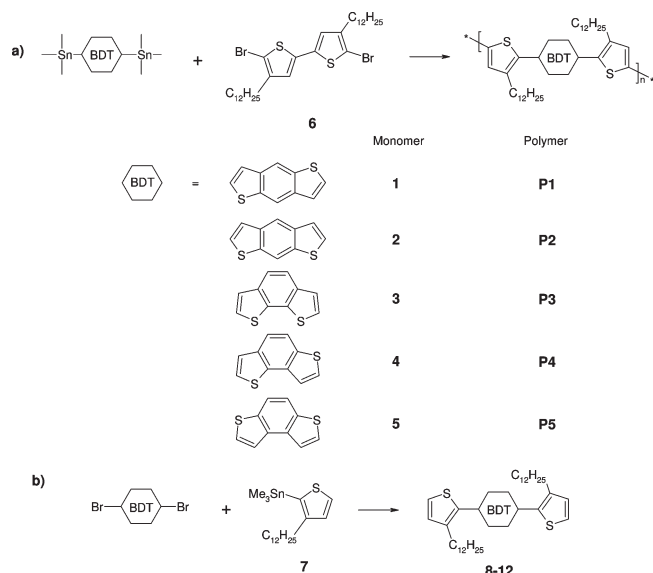
These polymers need to be well-soluble and efficiently pack with a high degree of order.^{10–13} It is thus of fundamental importance to better understand the relation between molecular structure and film morphology.^{14–16} In many cases, polymers with high tendency to pack into well-ordered films are sparingly soluble. Recently, we have reported on benzo[2,1-b;3,4-b']dithiophene (3) as new building block which renders a polymer with curved backbone.¹⁷ The high aggregation tendency of benzodithiophene directs the polymer to highly ordered films while the curvature within the polymer chain contributes to the solubility facilitating film formation. The curving of a conjugated polymer has already caused attention in the past, particularly for fluorene and carbazole containing polymers. Both monomers induce curvature because of their nonlinear geometry.^{18–20} Various modifications on these monomers have been studied to understand the impact of backbone curvature on the packing. For example, fluorene has been fused with another indene unit to reverse the monomer bending yielding a linear building block.²¹

As polymers structurally similar to polythiophene are particularly important conductive materials in electronic devices, it is crucial to understand the relationship between the molecular structure and the bulk properties for this particular class of polymers. For this reason, we present a full series of five isomeric polymers containing

*Corresponding author. E-mail: muellen@mpip-mainz.mpg.de.

- (1) de Boer, B.; Facchetti, A. *Polym. Rev.* **2008**, *48*, 423–431.
- (2) Coropceanu, V.; Cornil, J.; da Silva, D. A.; Olivier, Y.; Silbey, R.; Brédas, J. L. *Chem. Rev.* **2007**, *107*, 926–952.
- (3) Sirringhaus, H.; Ando, M. *MRS Bull.* **2008**, *33*, 676–682.
- (4) Anthony, J. E.; Heeney, M.; Ong, B. S. *MRS Bull.* **2008**, *33*, 698–705.
- (5) Sirringhaus, H. *Adv. Mater.* **2005**, *17*, 2411–2425.
- (6) Ong, B. S.; Wu, Y. L.; Li, Y. N.; Liu, P.; Pan, H. L. *Chem.—Eur. J.* **2008**, *14*, 4766–4778.
- (7) Berggren, M.; Nilsson, D.; Robinson, N. D. *Nat. Mater.* **2007**, *6*, 3–5.
- (8) Noh, Y. Y.; Zhao, N.; Caironi, M.; Sirringhaus, H. *Nat. Nanotechnol.* **2007**, *2*, 784–789.
- (9) Allard, S.; Forster, M.; Souharce, B.; Thiem, H.; Scherf, U. *Angew. Chem., Int. Ed.* **2008**, *47*, 4070–4098.
- (10) Chabinc, M. L.; Jimison, L. H.; Rivnay, J.; Salleo, A. *MRS Bull.* **2008**, *33*, 683–689.
- (11) Fong, H. H.; Pozdin, V. A.; Amassian, A.; Malliaras, G. G.; Smilgies, D. M.; He, M. Q.; Gasper, S.; Zhang, F.; Sorensen, M. *J. Am. Chem. Soc.* **2008**, *130*, 13202–13203.
- (12) DeLongchamp, D. M.; Kline, R. J.; Lin, E. K.; Fischer, D. A.; Richter, L. J.; Lucas, L. A.; Heeney, M.; McCulloch, I.; Northrup, J. E. *Adv. Mater.* **2007**, *19*, 833–837.
- (13) Surin, M.; Leclere, P.; Lazzaroni, R.; Yuen, J. D.; Wang, G.; Moses, D.; Heeger, A. J.; Cho, S.; Lee, K. *J. Appl. Phys.* **2006**, *100*, 33712.

- (14) Koch, N. *Chem. Phys. Chem.* **2007**, *8*, 1438–1455.
- (15) Shen, Y. L.; Hosseini, A. R.; Wong, M. H.; Malliaras, G. G. *ChemPhysChem* **2004**, *5*, 16–25.
- (16) Kline, R. J.; McGehee, M. D. *Polym. Rev.* **2006**, *46*, 27–45.
- (17) Rieger, R.; Beckmann, D.; Pisula, W.; Steffen, W.; Kastler, M.; Müllen, K. *Adv. Mater.* **2010**, *22*, 83–86.
- (18) Li, J. L.; Dierschke, F.; Wu, J. S.; Grimsdale, A. C.; Müllen, K. *J. Mater. Chem.* **2006**, *16*, 96–100.
- (19) Scherf, U.; List, E. J. W. *Adv. Mater.* **2002**, *14*, 477–481.
- (20) Chua, L. L.; Zaumseil, J.; Chang, J. F.; Ou, E. C. W.; Ho, P. K. H.; Sirringhaus, H.; Friend, R. H. *Nature* **2005**, *434*, 194–199.
- (21) Setayesh, S.; Marsitzky, D.; Müllen, K. *Macromolecules* **2000**, *33*, 2016–2020.

Scheme 1. (a) Polymer Synthesis;^a (b) Synthesis of the Repeat Unit (8–12) As Reference^b

^a Conditions: Pd₂(dba)₃, P(*o*-tol)₃, *o*-dichlorobenzene, 140 °C, 3 days.

^b Conditions: Pd(PPh₃)₄, DMF, 100 °C, overnight.

b-fused benzodithiophenes (**1–5**) with alkylated dithiophene (**6**) as comonomer. Because of the different bond geometry in the benzodithiophene monomers, different degrees of backbone curvature are designed. The goal of this work is to study the impact of these geometrical differences on both the molecular energy levels and the packing behavior of the polymers in bulk material. These results are correlated with the charge-carrier mobility of the polymers in organic field-effect transistors in order to get information on how to design new and even more effective semiconducting polymers.

Experimental Section

The benzodithiophenes were synthesized according to procedures described in the literature.^{22–24} They were stannylated by double lithiation with *t*-butyllithium at –78 °C and subsequent treatment with trimethyltin chloride. The crude products were subjected to reverse phase chromatography on RP18 silica gel (Sigma-Aldrich) and crystallized from acetonitrile to achieve the high purity needed for step growth polymerizations. The purity was verified by ¹H NMR, ¹³C NMR, and elemental analysis (for details, refer to the Supporting Information).

Dibromo-didodecyl-dithiophene (**6**) was synthesized according to the literature procedure and purified by repeated crystallization from ethyl acetate until very high purity was reached.²⁵

The polymers (**P1–P5**) were synthesized all under the same conditions by a Stille polymerization (compare Scheme 1). The bisstannylated benzodithiophene (**1–5**) and dialkyl-dibromodithiophene (**6**) were dissolved in degassed anhydrous *o*-dichlorobenzene, Pd₂(dba)₃, and triphenylphosphine were added as

catalyst system. After three days at 140 °C, the polymers were precipitated in methanol and subjected to Soxhlet extraction with acetone to remove residual catalyst and low molecular weight material.

The reference molecules (**8–12**) resembling the repeat unit of the polymer **P1–P5** were synthesized from the brominated benzodithiophenes in a Stille reaction. The corresponding dibromide was dissolved in anhydrous DMF under argon, dodecyl-trimethylstannylthiophene (**7**) and Pd(PPh₃)₄ were added and heated overnight to 100 °C. The molecules were isolated by preparative chromatography on silica gel.

The UV–vis absorption spectra were recorded in a 1 × 10^{–4} M (with regard to the repeat unit) solution in *o*-dichlorobenzene on a Perkin-Elmer Lambda 100 spectrophotometer. For the high-temperature measurements, the cuvettes were heated to 100 °C by a heat gun and immediately measured. The film measurements were performed by drop-casting an *o*-dichlorobenzene solution on a quartz glass and using the same instrument. Photoluminescence in 1 × 10^{–4} M *o*-dichlorobenzene solution were recorded on a SPEX-Fluorolog II (212) instrument.

Cyclic voltammetry was measured on a Princeton Applied Research Parstat 2273 instrument with anhydrous acetonitrile under argon atmosphere. Tetrabutylammonium perchlorate was used as conductive salt at a concentration of 0.1 mol/L. Ferrocene was added as internal standard (1 mM). A small drop of the polymer dissolved in dichlorobenzene was put on a platinum working electrode (0.5 mm diameter) and evaporated, a platinum wire as counter electrode, and a silver wire as quasi-reference electrode were used. The peaks were calibrated according to the oxidation peak of ferrocene. The voltage was scanned by 100 mV/s. Half-step potentials were used for the evaluation.

The two-dimensional wide-angle X-ray diffraction experiments were performed by means of a rotating anode (Rigaku 18 kW) X-ray beam with a pinhole collimation and a 2D Siemens detector with a beam diameter of ca. 1 mm. A double graphite monochromator for the Cu–K_α radiation (λ = 0.154 nm) was used.

For the field-effect transistor measurements, highly doped silicon including a 200 nm thick thermally grown SiO₂ film was used as substrate. The substrates were silanized using HMDS by vapor deposition (resulting in contact angles of 93.2 ± 1.3°) or octadecyltrichlorosilane (OTS) by vapor deposition (resulting in contact angles of 110.4 ± 1.0°). In addition, polymeric dielectrics like benzocyclobutene (BCB) or Cytop were used.

A series of bottom contact bottom gate FETs (channel length 5–100 μm and width 0.35 to 7.0 mm, W/L = 70) and top contact bottom gate FETs (channel length 25–75 μm and width 0.5 to 1.5 mm, W/L = 20) were prepared by drop-casting and spin-coating hot 5 mg/mL dichlorobenzene solutions.

Solution processing and electrical measurements by using a Keithley 4200 machine were performed inside a nitrogen filled glovebox (oxygen < 1.2 ppm, humidity < 0.1 ppm, pressure ~1120 Pa) at room temperature (~25 °C).

The charge carrier mobility was calculated in saturation from the equation

$$\mu_{\text{sat}} = \frac{2I_{\text{SD}}L}{WC_i(V_{\text{SG}} - V_{\text{th}})^2}$$

Results and Discussion

To analyze the geometry of the newly synthesized polymers in more detail, the molecular structure of the benzodithiophene monomers and the resulting polymer

(22) Takimiya, K.; Konda, Y.; Ebata, H.; Niihara, N.; Otsubo, T. *J. Org. Chem.* **2005**, *70*, 10569–10571.

(23) Yoshida, S.; Fujii, M.; Aso, Y.; Otsubo, T.; Ogura, F. *J. Org. Chem.* **1994**, *59*, 3077–3081.

(24) Archer, W. J.; Cook, R.; Taylor, R. *J. Chem. Soc. Perkin Trans. 2* **1983**, 813–819.

(25) Heeney, M.; Bailey, C.; Genevicius, K.; Shkunov, M.; Sparrowe, D.; Tierney, S.; McCulloch, I. *J. Am. Chem. Soc.* **2005**, *127*, 1078–1079.

backbones are simulated by a force-field optimization using MMFF (see Table 1). The monomer angle shall be the angle the benzodithiophene would introduce into an otherwise linear polymer. The lower this value, the more curvature is present in the polymer chain. These are depicted in the center of Table 1 together with a contour line fit. As the contour lines are sine-shaped, they offer the possibility to extract a wavelength and amplitude to quantify the degree of curvature; the values are presented on the right side of Table 1. The amplitude increases strongly from **P1** through **P5** in accordance with the qualitative pictures. For **P1**, the amplitude is nonzero, although the monomer does not introduce any curvature. The slight nonlinearity is due to the bithiophene, which itself is not strictly linear. Its contribution, however, becomes negligible for the more strongly curved polymers **P2–P5**. With increased amplitude the wavelengths of the contour lines become shorter. It is thus also a measure of the curvature. The only exception is **P1** in which the wavelength is much shorter; the wavelength is about half of that of **P2**. The reason for this is that only the bithiophene causes a small curvature, whereas the benzodithiophene does not; it is perfectly linear. In the following, the expression “strong curvature” shall therefore refer to a high amplitude of the contour line of the polymer backbone.

The molecular weights of the polymers as determined by size exclusion chromatography are almost identical for **P1–P3** (Table 2). For the more strongly curved polymers **P4** and **P5**, lower values are obtained. This may be due to

Table 1. Geometry of the Polymers: The Monomer Angle Refers to the Angle Which Is Introduced by the Corresponding Benzodithiophene into a Linear Polymer Chain. The Backbone Shows the Contour Lines of the Force-Field Optimized (MMFF) Polymer Chains from Which the Amplitude and Wavelength of the Chain Are Obtained

Polymer	Monomer Angle	Backbone	Amplitude	Wavelength
P1	180°		0.14 nm	1.47 nm
P2	169°		0.29 nm	2.82 nm
P3	127°		0.31 nm	2.83 nm
P4	113°		0.59 nm	2.75 nm
P5	106°		0.88 nm	2.32 nm

difficulties in the polymerization process, as these polymers have more freedom to fold back thus reducing the accessibility of the reactive chain ends for further addition reactions. On the other hand, the values may reflect a lower hydrodynamic radius of the more flexible polymers, leading to an apparently lower molecular weight in comparison to the other polymers. Nevertheless, a difference by a factor of 2 in molecular weights should not have a dramatic effect on the materials properties.

A significant trend within the present series becomes obvious when comparing the solubility of the polymers: the stronger the curvature becomes the better soluble is the polymer. Polymer **P1** dissolves only in dichlorobenzene at elevated temperatures (about 5 g/L at 100 °C), upon cooling to room temperature, it precipitates again even at concentrations below 1 g/L. In contrast, *o*-dichlorobenzene solutions of polymer **P5** are still stable at room temperature, exceeding 20 g/L. Furthermore, it even dissolves in toluene to about 10 g/L at room temperature. The solubility of the other polymers lies in between these limits. Polymer **P3** forms a gel when an *o*-dichlorobenzene solution is cooled to room temperature. This solubility trend is most likely the result of a stronger self-association of the rodlike polymers which can pack much more easily into lamellae in comparison to the curved ones. Also, the entropy gain of more strongly curved polymers upon dissolving is higher than for stiff polymers, which cannot easily form coils because of their rotational invariance.

The energy levels of the polymer series have been measured by UV–vis spectroscopy and cyclic voltammetry and are summarized in Table 2. The optical gaps determined by the onset of the UV–vis absorption peaks generally increase with increased degree of curvature, in particular for polymers **P1**, **P3**, and **P5**. For the stiff linear polymers, the conjugation length is obviously longer, thus the optical gap smaller. The higher the curvature, the shorter becomes the conjugation length. Consequently, the optical gap becomes wider.

However, polymers **P2** and **P4** do not strictly follow this trend as can be seen more clearly in the plot of Figure 1a. The absorption peaks are shifted hypsochromically when going from polymer **P1** over **P3** to **P5**. The absorption peaks of polymers **P2** and **P4** are shifted more hypsochromically than one would expect from the curvature dependence described above. The deviation has been marked by arrows on the right side of Figure 1a. A possible explanation could be a reduced conjugation

Table 2. Characterization of the Polymer Series

polymer	M_n^a (kg mol ⁻¹)	M_w^a (kg mol ⁻¹)	film λ_{\max} (nm)	E_g^b (eV) (UV)	$E_{1,ox}^c$ (eV) (CV)	$E_{2,ox}^c$ (eV) (CV)
P1	17	41	521	2.17	0.39	1.07
P2	21	49	471	2.49	0.48	0.84
P3	21	54	527	2.26	0.37	1.18
P4	11	25	460	2.53	0.63	0.92
P5	12	25	432	2.46	0.57	0.92

^a Molecular weight as determined by size exclusion chromatography in 1,2,4-trichlorobenzene at 135 °C against polystyrene standard. ^b Optical gap as determined from the onset of the UV–vis absorption in an *o*-dichlorobenzene solution. ^c Oxidation potentials against ferrocene measured by cyclic voltammetry of a polymer film on a platinum electrode immersed in an acetonitrile solution with Bu₄NClO₄ as electrolyte and ferrocene as internal reference.

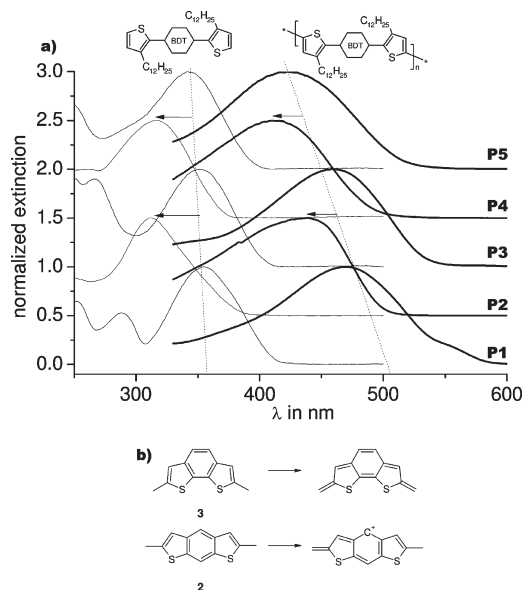


Figure 1. (a) Absorption spectrum of the model substances resembling the repeating units of the polymers in comparison to the corresponding polymers, recorded in *o*-dichlorobenzene at 1×10^{-4} M (for the polymers with regard to the repeat unit); (b) possibilities to quinodize for polymer **3** in contrast to monomer **2**.

through the benzodithiophene monomers. As indicated in Figure 1b, benzodithiophene **3** can quinodize upon oxidation. The same applies for benzodithiophene **1** and **5**. For benzodithiophene **2** and **4**, however, this quinodization is not possible because the sulfur atoms stand meta to the central benzene ring. This leads to a reduced conjugation and consequently to a further increase in the optical gap of the corresponding polymers in addition to the trend of a hypsochromic shift, which correlates to the degree of curvature.

To confirm that the deviation of the optical spectra of polymers **P2** and **P4** is not an effect of the polymer geometry, small molecules (**8–12**) representing the repeat units of the polymers have been synthesized as models and characterized by their optical absorption spectra. The result is displayed on the left of Figure 1a. As indicated by the broken line, the model molecules **8**, **10**, and **12**, which correspond to the repeat unit of polymers **P1**, **P3**, and **P5**, show their absorption maxima at about the same wavelength. This underlines that the different optical gaps in the polymers do not arise from electronic differences in the building blocks. The absorption maxima of model molecules **9** and **11**, corresponding to polymers **P2** and **P4**, are found at about 30 nm shorter wavelength as for **8**, **10**, and **12**. As expected, the monomers with sulfur atoms in the meta position to the central benzene ring possess a wider band gap themselves such that the corresponding polymers show absorption at lower wavelengths than the curvature trend would explain.

The hypsochromic shift upon stronger curvature is even more pronounced in the film. The absorption peak in the film UV–vis spectrum of the heavily curved polymer **P5** is by almost 100 nm blue-shifted in comparison to the almost linear isomer **P1**. Obviously, the aggregation tendency, which gives rise to absorption bands at longer

Table 3. Morphology Investigations by Fiber X-ray Scattering and the Performance in Field-Effect Transistors on Silicon Substrates with a Top-Contact Bottom-Gate Setup

polymer	$d_{\pi-\pi}^a$ (nm)	d_{lam}^b (nm)	μ_{sat}^c ($\text{cm}^2 \text{V}^{-1} \text{s}^{-1}$)	$I_{\text{on}}/I_{\text{off}}^d$
P1	0.37	1.9	1.5×10^{-2}	9.1×10^4
P2	0.37	1.9	1.8×10^{-3}	5.3×10^3
P3	0.37	1.9	0.13	1.9×10^5
P4	0.37	3.1	3.0×10^{-4}	6.8×10^2
P5	0.38	2.9	1.8×10^{-4}	2.0×10^3

^a π -Stacking distance. ^b Lamellar distance. ^c Saturation field-effect mobility. ^d On–off ratio.

wavelengths is responsible for this observation.²⁶ However, the trend is not as clear as in solution, as other effects arising from intermolecular interactions also play a role in the bulk material. Polymer **P3** shows a peak at the largest wavelength in the film.

The first oxidation peak in film cyclic voltammetry follows a very similar trend as the film absorption peaks. In general, the stronger the curvature, the higher is the oxidation potential. This is consistent with the assumption of a reduced conjugation length as described above for the optical gap. The meta effect described above for **P2** and **P4** can be found here again. Polymer **P3** can be oxidized a bit more easily than the trend would imply. A very efficient packing leading to stabilization of the positive charge by the neighboring chain may be the reason.

For more information on the bulk morphology of the polymer series, the materials have been extruded as a fiber. The two-dimensional diffraction of an X-ray beam reveals both the π -stacking distance and the packing mode. It is not surprising that all polymers form lamellae like most other alkyl-substituted polythiophenes do as well.¹⁶ As summarized in Table 3, the π -stacking distance is basically unaffected by the extent of curvature in the polymer. In all cases, a value between 0.37 and 0.38 nm is found. This value is about the same as in polymers with the highest charge-carrier mobility.^{27–29} The extended benzodithiophene obviously brings the chains close together no matter how the geometry of the polymer looks like.

The interlamellar distance, however, is much higher for the highly curved polymers **P4** and **P5** than for the others. Structure models obtained from force-field optimizations suggest that the alkyl chains on the bent polymer backbones cannot interdigitate as effectively as for the almost linear polymers. The qualitative trend of lower order on increased backbone curvature as estimated from the half-width of the X-ray diffraction peaks stands in good agreement to this observation.

- (26) Yamamoto, T.; Komarudin, D.; Arai, M.; Lee, B. L.; Suganuma, H.; Asakawa, N.; Inoue, Y.; Kubota, K.; Sasaki, S.; Fukuda, T.; Matsuda, H. *J. Am. Chem. Soc.* **1998**, *120*, 2047–2058.
- (27) Prosa, T. J.; Winokur, M. J.; Moulton, J.; Smith, P.; Heeger, A. J. *Macromolecules* **1992**, *25*, 4364–4372.
- (28) Tsao, H. N.; Cho, D.; Andreasen, J. W.; Rouhanipour, A.; Breiby, D. W.; Pisula, W.; Müllen, K. *Adv. Mater.* **2009**, *21*, 209–212.
- (29) McCulloch, I.; Heeney, M.; Bailey, C.; Genevicius, K.; Macdonald, I.; Shkunov, M.; Sparrowe, D.; Tierney, S.; Wagner, R.; Zhang, W. M.; Chabinyc, M. L.; Kline, R. J.; McGehee, M. D.; Toney, M. F. *Nat. Mater.* **2006**, *5*, 328–333.

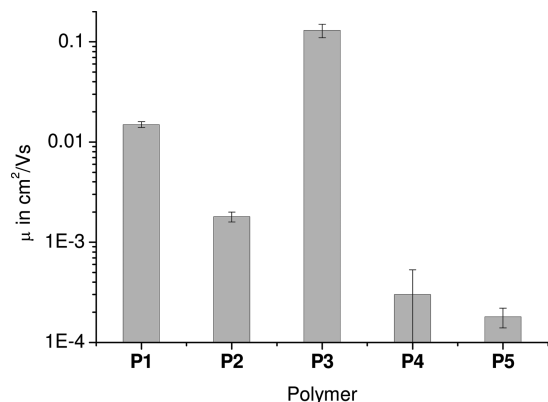


Figure 2. Plot of the hole field-effect mobility of the polymer series.

The charge-carrier mobility of the polymer series has been measured on a top-contact bottom-gate transistor setup. A highly doped silicon wafer with a silicon dioxide layer has been treated with hexamethyldisilazane (HMDS). The polymer is spin-cast on top from a *o*-dichlorobenzene solution. Finally, gold electrodes are evaporated. The results are summarized on the right side of Table 3. The highest mobility is measured for polymer **P3** exhibiting an intermediate degree of curvature. Both for lower and for higher curvatures, the mobility goes down. The linear isomer is so poorly soluble that the fabrication is difficult as precipitation competes with film formation. This hinders the formation of a uniform film with high degree of order at the interface to the gate dielectric. Thermal annealing cannot fully recover the defects, the chains are probably too stiff. As a very similar polymer has shown higher mobility values,³⁰ the intrinsic mobility might be much higher than measured here, but very hard to reach in practice.

For the higher curvature, the mobility goes down relative to polymer **P3** due to the low order and thus unfavorable film formation propensity. The relatively high flexibility of the polymer chains upon bond rotation makes it unlikely to create long-range order in a film. A thermal annealing does not favor higher order, as the

enthalpy gain upon crystallization cannot easily compensate the significant entropy loss.

As for the UV–vis studies, the two polymers **P2** and **P4** do not strictly follow the trend because of their lowered backbone conjugation. The lack of a quinodized structure as outlined in Figure 2b is obviously detrimental to the charge-carrier transport along the polymer chain. A lower mobility than expected by the trend line in Figure 2 is thus plausible. The deviation from the trend is on the same order of magnitude on the logarithmic scale. This means that polymer **P3**, bearing the sulfur atoms in the favorable ortho position with regard to the benzene ring, represents the optimum compromise between high order for good charge-carrier mobility and sufficient solubility for efficient film formation from solution.

Summary

In summary, an isomeric series of benzodithiophene containing polythiophenes have been synthesized with different degrees of curvature along the polymer backbone. By UV–vis spectroscopy, it has been shown that the optical gap increases with increasing curvature, probably because of a reduced effective conjugation length of the polymer. The conjugation of monomers **2** and **4**, in which the sulfur atoms are arranged meta with regard to the benzene unit, is reduced, leading to an increased band gap. The order in bulk is reduced by increasing the curvature, but the π -stacking distance remains unaffected. The field-effect measurements show that the moderately curved polymer **P3** possesses the highest mobility. It exhibits high order and good solubility. The more highly curved polymers show reduced order in the film, whereas the less curved have too low solubility for processing. For further developments in the field, the backbone geometry of conjugated polymers should be considered to design new materials with even superior performance.

Supporting Information Available: Experimental procedures, analytical data for all new compounds, and details on the measurements (PDF). This material is available free of charge via the Internet at <http://pubs.acs.org>.

(30) Pan, H. L.; Li, Y. N.; Wu, Y. L.; Liu, P.; Ong, B. S.; Zhu, S. P.; Xu, G. *J. Am. Chem. Soc.* **2007**, *129*, 4112–4113.